



### **Science Arts & Métiers (SAM)**

is an open access repository that collects the work of Arts et Métiers Institute of Technology researchers and makes it freely available over the web where possible.

This is an author-deposited version published in: <https://sam.ensam.eu>  
Handle ID: <http://hdl.handle.net/10985/10558>

#### **To cite this version :**

René ROTINAT, Raphaël MOULART, François NUNIO, Pierre VEDRINE - Experimental identification of the overall elastic rigidities of superconducting windings - International Journal of Applied Electromagnetics and Mechanics p.1-6 - 2016

Any correspondence concerning this service should be sent to the repository

Administrator : [scienceouverte@ensam.eu](mailto:scienceouverte@ensam.eu)



# Experimental identification of the overall elastic rigidities of superconducting windings

René Rotinat <sup>a,\*</sup>, Raphaël Moulart <sup>a</sup>, François Nunio <sup>b</sup> and Pierre Vedrine <sup>b</sup>

<sup>a</sup> *MSMP lab., Arts et Métiers ParisTech, Rue St Dominique, BP 508, Châlons-en-Champagne Cedex, F-51006, France*

<sup>b</sup> *DSM/IRFU, CEA, Bâtiment 123, Gif-sur-Yvette Cedex, F-91191, France*

**Abstract.** This study deals with an experimental methodology developed in order to identify the elastic properties of superconducting ring-shaped windings, constituents of the main coil winding of a magnetic resonance imaging magnet (MRI). Mechanical tensile tests were conducted on real scale specimens associated to an optical full-field displacement measurement technique (stereo image correlation). Strain fields were then obtained from the measured displacement fields by numerical differentiation. Finally, the four in-plane orthotropic stiffnesses of the windings were determined using the Virtual Fields Method (VFM). Experimental set-up also allows detecting a possible occurrence of a delamination thanks to in-plane displacement fields.

Keywords: Full-field measurement, DIC, orthotropic elasticity, VFM, superconductors, MRI

## 1. Introduction

The objective of the French-German project Iseult / INUMAC is to develop a whole-body 11.7 T magnetic resonance imaging device (MRI) to improve sensitivity, spatial, temporal and spectral resolution for preclinical and clinical MRI system [1]. This 900 mm bore, very high field whole body magnet, is being developed on the basis of Niobium-Titanium (NbTi) superconductors (cf. Fig. 1(a)). The superconducting magnet will be housed in a massive cryostat weighting some 132 t. When energized, 338 MJ will be stored in the magnetic field.

The main coil winding (cf. Fig. 1(b)) is a stack of double pancakes (DP) composed of two layers connected through a transition area (cf. Fig. 1(c)). Copper/NbTi cable-in-channel-type conductor is wound in  $2 \times 88$  turns in each DP and insulation fiberglass-epoxy composite tape bonds the conductors together. A fiberglass-epoxy composite plate is inserted between the two coil layers for insulation, and an additional fiberglass-epoxy composite plate is attached on the inner diameter area of the DP. The manufacturing of large superconducting magnets makes it necessary to determine accurately their elastic properties.

The mechanical properties of coil winding are usually obtained from mechanical tests given homogeneous stress fields in the specimens and using local measurement techniques through strain gauges

---

\*Corresponding author: First Author, MSMP lab., Arts et Métiers ParisTech, Rue St Dominique, BP 508, Châlons-en-Champagne, F-51006, France,  
E-mail: rene.rotinat@ensam.eu

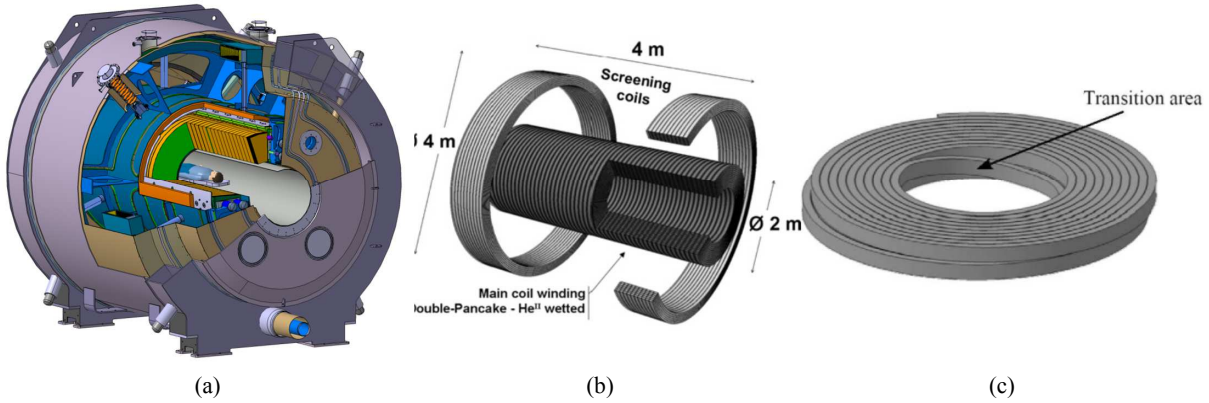


Fig. 1. Iseult MRI: (a) Cut-away view of the magnet and cryostat assembly, (b) main coil winding and (c) geometry of the DP

[2,3]. However, these standard stiffness measurement techniques are unsuitable in the case of anisotropic materials such as superconducting windings.

This work aims at developing an experimental methodology based on non-contact full-field kinematic measurements and inverse identification procedure in order to identify equivalent elastic orthotropic stiffness components for this complex structure. In a previous work, a general methodology based on the use of the virtual fields method (VFM) to identify rigidities of thick laminated composite tubes has been firstly developed [4] then applied to a monolithic-type conductor DP [5] and finally to a reduced scale DP ( $2 \times 20$  turns winding) [6]. The objective of this present study, is to adapt this methodology to a real scale DP.

It has to be noted that the material constituents themselves (Copper/NbTi cables, fiberglass-epoxy tape, . . . ) are to be used in their elastic domain. Consequently, in this study, the DP structure is considered as a homogeneous equivalent material with a linear elastic constitutive equation.

## 2. Methodology

### 2.1. Mechanical test

The mechanical test on double pancakes is a diametrical tensile test, i.e. an actuator applies a force on two points of the inner radius of the DP leading to a mixed tensile-bending state of stress. A load cell, placed between the frame and the actuator measure the load information during the test. The experimental set-up is illustrated in Figure 2. A set of six CCD cameras (three for each side, see figure 2(a)), has been used to measure the deformation of the DP on both sides at the same time by stereo digital image correlation technique (DIC).

On each side of DP, two cameras (1-2 for side A and 4-5 for side B) follow in-plane and out-of-plane displacement of a partial DP area (a disk sector of  $30^\circ$ ) in order to extract rigidities (cf. Fig. 4). These four cameras used are 16-bit  $2048 \times 2048$  pixels CCD cameras. Two other cameras are employed on each side (3 for side A and 6 for side B) to track occurrence of delamination on the whole surface of the double pancake. The cameras used are a 16-bit  $4000 \times 2672$  pixels for camera 3 and a 12-bit  $1024 \times 1024$  pixels for camera 6.

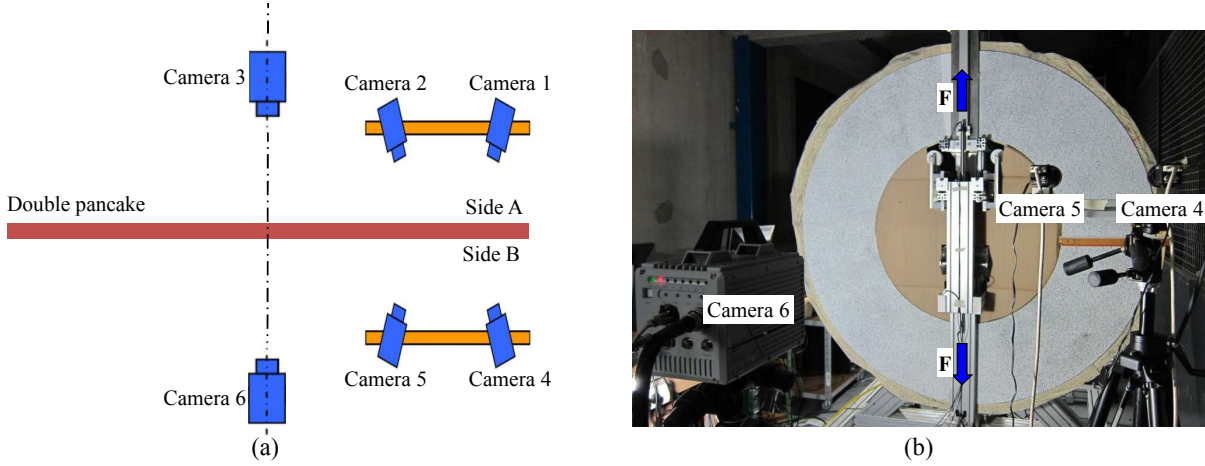


Fig. 2. Experimental set-up: (a) scheme and (b) picture of one side

To use the DIC technique, it is necessary to apply a speckle pattern onto the surface to study. This is done by spraying black paint on a previously uniformly white painted on both faces of the DP. The surfaces of the double pancake were smoothed down before applying the paint thanks to sand paper.

The experimental implementation was performed by VIC3D (see [www.correlatedsolutions.com](http://www.correlatedsolutions.com)) stereo-correlation software and the camera calibration was conducted for each face measurement [7,8]. The two stereovision systems have been calibrated using a target with  $12 \times 15$  points spaced by  $15 \text{ mm}$ . The in-plane displacement resolution obtained is closed to  $5 \times 10^{-3}$  pixels ( $0,002 \text{ mm}$ ) with a subset size equal to 26 pixels. The displacement fields measured on the two faces are illustrated on figure 3 for a load value of approximately  $150 \text{ kN}$ . The maps on the first column represent the displacement fields of the face A and the second column corresponds to the side B. X, Y and Z directions correspond to respectively the horizontal direction, the vertical direction and out-of-plane direction. Displacement fields obtained by DIC are then smoothed using a polynomial fitting algorithm [9]. Finally, the displacement fields were numerically differentiated to retrieve the three in-plane strain components.

## 2.2. Application of the virtual fields method

The Virtual Fields Method (VFM) is a method that allows to identify the stiffnesses of a material. It was introduced in 1989 by Grédiac [10,11] and is based on the principle of the virtual work. This one is itself based on the expression of the local equilibrium that can be written, in statics:

$$\overrightarrow{\text{div}} \bar{\sigma} + \bar{f} = 0 \quad (1)$$

Introducing a “virtual displacement field”  $\bar{u}^*$  (kinematically admissible), and an associated “virtual strain field”  $\bar{\varepsilon}^*$ , one can write this local equilibrium in an integral form, this is the so called “principle of virtual work”:

$$-\int_V \bar{\sigma} : \bar{\varepsilon}^* dV + \int_{\partial V_F} \bar{T} \cdot \bar{u}^* dS + \int_V \bar{f} \cdot \bar{u}^* dV = 0 \quad (2)$$

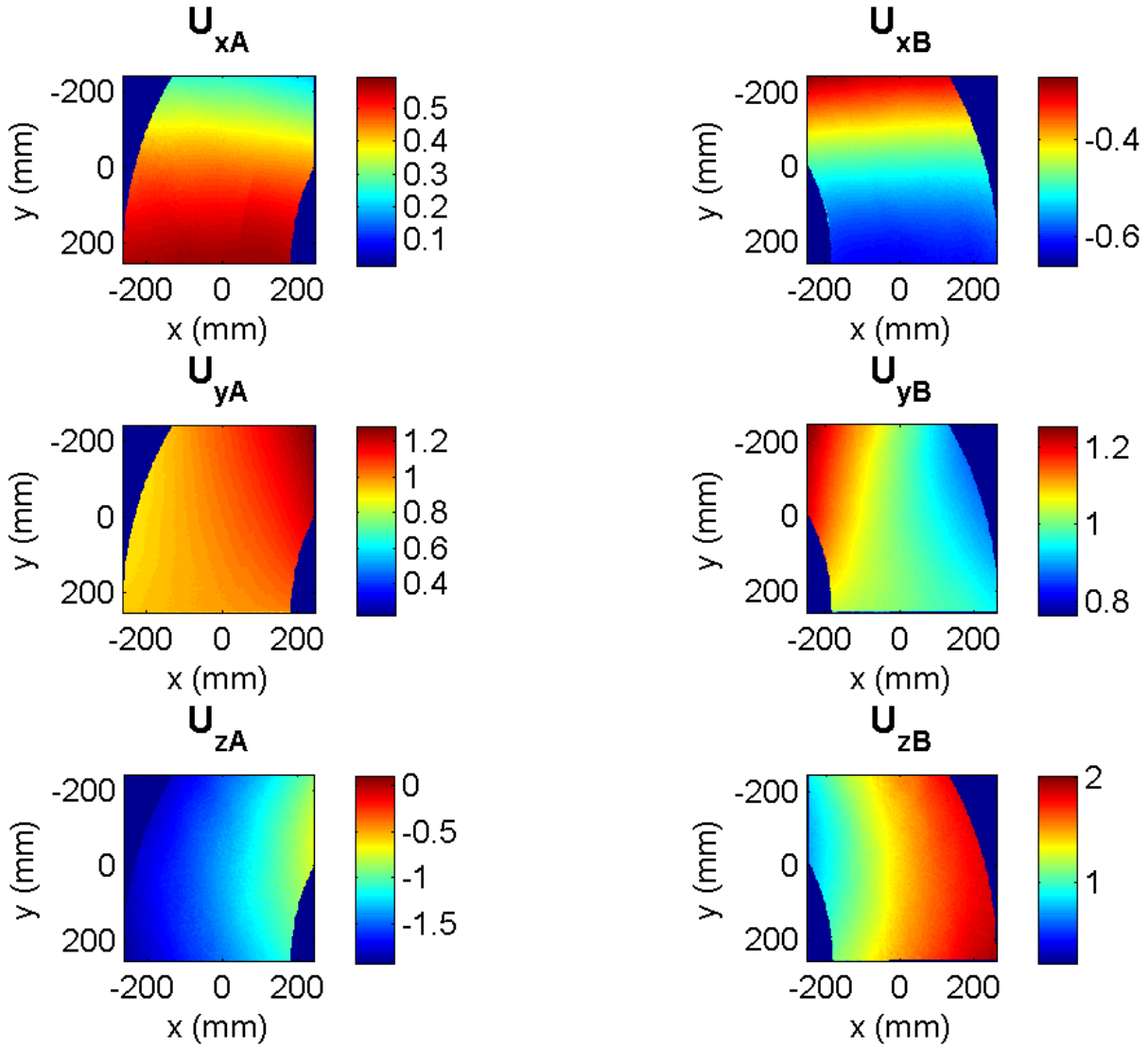


Fig. 3. Displacement maps at 149.25 kN load

where  $\vec{T}$  are the surface loadings and  $\vec{f}$  are the volumic loadings. Generally, one can neglect the volumic forces. This is especially the case for the winding since there is no volumic Laplace forces during the mechanical test as no volumic current is put in it. So, equation 2 can be re-written:

$$\int_V \bar{\sigma} : \bar{\varepsilon}^* dV = \int_{\partial V_F} \vec{T} \cdot \vec{u}^* dS \quad (3)$$

To be useful for identification purposes, the virtual displacement fields have to fulfil two conditions (summarized in figure 4(b)):

- to be kinematically admissible *i.e.* to be equal to the actual displacement field (generally, 0) on  $\partial V_U$ , portion of the boundary of the studied solid that is kinematically constrained;

- to be defined so as to make work only the resultant of the surface loadings since one does not know the exact repartition of these loadings.

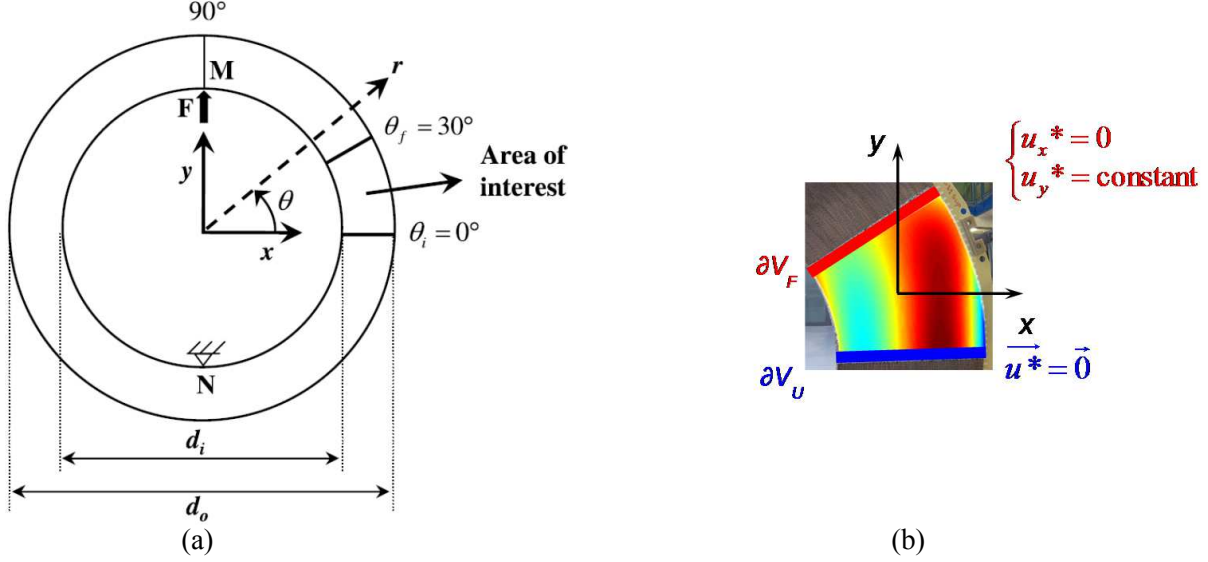


Fig. 4. DP configuration: (a) area of interest and (b) special conditions for the virtual displacement fields

This way, equation 3 becomes:

$$\int_V \bar{\sigma} : \bar{\varepsilon}^* dV = \text{constant} \times \int_{\partial V_F} \vec{T} dS = \text{constant} \times F_y \quad (4)$$

If the mechanical sollicitation leads to a plane stress state, it becomes:

$$e \int_S \bar{\sigma} : \bar{\varepsilon}^* dS = \text{constant} \times F_y \quad (5)$$

Introducing the orthotropic elastic constitutive equation (in polar coordinates), the terms of  $\bar{\sigma}$  are replaced by their value depending on the measured strains. Using the Voigt convention, this constitutive equation is:

$$\begin{Bmatrix} \sigma_r \\ \sigma_\theta \\ \sigma_s \end{Bmatrix} = \begin{bmatrix} Q_{rr} & Q_{r\theta} & 0 \\ Q_{r\theta} & Q_{\theta\theta} & 0 \\ 0 & 0 & Q_{ss} \end{bmatrix} \begin{Bmatrix} \varepsilon_r \\ \varepsilon_\theta \\ \varepsilon_s \end{Bmatrix} \quad (6)$$

This finally leads to:

$$Q_{rr} \int_S \varepsilon_r \varepsilon_r^* dS + Q_{\theta\theta} \int_S \varepsilon_\theta \varepsilon_\theta^* dS + Q_{r\theta} \int_S (\varepsilon_\theta \varepsilon_r^* + \varepsilon_r \varepsilon_\theta^*) dS + Q_{ss} \int_S \varepsilon_s \varepsilon_s^* dS = \frac{\text{constant} \times F_y}{e} \quad (7)$$

One single virtual displacement field leads to one equation. As there are four unknowns (the  $Q_{ij}$ ), four equations, and so, four virtual fields, are needed. Assuming that these fields are chosen such as the equations are independent, this leads to a linear system of four equations with four unknowns that can

Table 1  
Identified and reference stiffness components for double pancakes

Rigidities	Identified		Reference
	Mean	Standard deviation	
$E_{rr}$	86.7	7.8	82
$E_{\theta\theta}$	116.7	3.5	115
$G_{ss}$	21.3	1.1	29
$\nu_{\theta r}$	0.38	0.004	0.36

be inverted so as to identify the four orthotropic stiffnesses. More details about the VFM can be found in this article [11].

### 3. Results and discussion

The preliminary study [6] has proven that, due to the complex structure of the windings, out-of-plane bending occur when submitted to the diametral tension and that it is necessary for a correct identification of stiffnesses to cancel it by averaging strain fields from both sides of the DP. These average strain fields are then computed by VFM technique [4]. As expected, the  $Uz$  displacement measured on one face (see figure 3) is equal to the one measured on the other face with an opposite sign. The maximum out-of-plane deflection is observed in the outer radius at the middle section.

The average identified values are listed in Table 1<sup>1</sup>. The identification of  $E_{\theta\theta}$ ,  $G_{ss}$  and  $\nu_{\theta r}$  is reasonably stable. A larger spread is observed for  $E_{rr}$  because this stiffness is related to the radial strain which is very low due to the way the structure is solicited. Reference stiffness values (Table 1) can be calculated by considering a finite elements numerical procedure. The computation process is conducted following a classical homogenization procedure [13], based on micro-mechanical analysis. A Representative Unit Cell (RUC) of the winding, which captures the major features of its underlying macro-structure is modeled. The homogenized constitutive law of the RUC can be determined from the known properties of its constituents (superconductor, insulation tape), solving six independents elastic problems. It was observed that experimental results are in good agreement with these reference values.

Displacements on whole side A measured with a spatial resolution closed to 0.5 mm have shown the occurrence of delamination when the load reaches 160 kN. However, displacements on whole side B measured with a spatial resolution of about 1.7 mm have failed to see this phenomenon.

### 4. Conclusion

In conclusion, the methodology associating a non-contact full-field measurement technique and an inverse identification procedure (VFM) to process strain fields allows to identify the overall elastic rigidities of the real scale DP forming the main coil winding. The set-up developed also allows to control in the same time the appearance of delamination cracks upon the suitability of spatial resolution.

<sup>1</sup>The links between the rigidities appearing in equations 6 and 7 and the modulus given in Table 1 come from plane-stress state hypothesis. These are:  $Q_{rr} = E_{rr}/(1 - \nu_{\theta r}\nu_{r\theta})$ ;  $Q_{\theta\theta} = E_{\theta\theta}/(1 - \nu_{\theta r}\nu_{r\theta})$ ;  $Q_{r\theta} = \nu_{\theta r}E_{rr}/(1 - \nu_{\theta r}\nu_{r\theta})$ ;  $Q_{ss} = G_{r\theta}$ ;  $\nu_{r\theta} = \nu_{\theta r}E_{rr}/E_{\theta\theta}$ .

## References

- [1] P. Vadrine, G. Aubert, F. Beaudet, J. Belorgey, J. Beltramelli, C. Berriaud, P. Bredy, P. Chesny, A. Donati, G. Gilgrass, G. Grunblatt, F.P. Juster, F. Molinie, C. Meuris, F. Nunio, A. Payn, L. Quettier, J.M. Rey, T. Schild, A. Sinanna, The Whole Body 11.7 T MRI Magnet for Iseult/INUMAC Project, *IEEE Trans. Appl. Supercond.*, **18** (2008), 868–873.
- [2] I.R. Dixon, R.P. Walsh and W.D. Markiewicz, Mechanical properties of epoxy impregnated superconducting solenoids, *IEEE Trans. Magn.*, **32** (1996), 2917–2920.
- [3] H. Nakajima, K. Yoshida and Y. Hatori, Structural behavior of winding and superconductor under mechanical loading, *IEEE Trans. Magn.*, **23** (1987), 1521–1524.
- [4] R. Moulart, S. Avril and F. Pierron, Identification of the through-thickness rigidities of a thick laminated composite tube, *Composite A*, **37** (2006), 326–336.
- [5] J.-H. Kim, F. Nunio, F. Pierron and P. Vadrine, Identification of the mechanical properties of superconducting using the virtual fields method, *IEEE Trans. Appl. Supercond.*, **24** (2010), 1993–1997.
- [6] J.-H. Kim, F. Nunio, F. Pierron and P. Vadrine, Characterizing elastic properties of superconducting windings by simulations and experiments, *Supercond. Sci. Technol.*, **24** (2011), 125001 (15pp).
- [7] M.A. Sutton, J. H. Yan, V. Tiwari, H. W. Schreier and J.-J. Orteu, The effect of out-of-plane motion on 2D and 3D digital image correlation measurements, *Opt. Lasers Eng.*, **46** (2008), 746–757.
- [8] F. Amiot, M. Bornert, P. Doumalin, J.-C. Dupré, M. Fazzini, J.-J. Orteu, C. Poilâne, L. Robert, R. Rotinat, E. Toussaint, B. Wattrisse and J.S. Wienin, Assessment of Digital Image Correlation Measurement Accuracy in the Ultimate Error Regime: Main Results of a Collaborative Benchmark, *Strain*, **49** (2013), 483–496.
- [9] Y. Pannier, S. Avril, R. Rotinat and F. Pierron, Identification of elastoplastic constitutive parameters from statically undetermined tests using the virtual fields method, *Exp. Mech.*, **46** (2006), 735–755.
- [10] M. Grédiac, Principe des travaux virtuels et identification, *Mécanique des Solides – Comptes rendus de l’Académie des Sciences*, **309** (1989), (in French with abridged English version).
- [11] M. Grédiac and F. Pierron and S. Avril and E. Toussaint, The Virtual Fields Method for Extracting Constitutive Parameters From Full-Field Measurements: a Review, *Strain*, **42** (2006), 233–253.
- [12] Y. Pannier, S. Avril, R. Rotinat and F. Pierron, Identification of elastoplastic constitutive parameters from statically undetermined tests using the virtual fields method, *Exp. Mech.*, **46** (2006), 735–755.
- [13] H. Berger, S. Kurukuri, S. Kari, U. Gabbert, R. Rodriguez-Ramos, J. Bravo-Castillero and R. Guinovart-Diaz, Numerical and analytical approaches for calculating the effective thermo-mechanical properties of three-phase composites, *Journal of Thermal Stresses*, **30** (2007), 801–817.